Title

Real-Time Monitoring of Alzheimer's-Related Amyloid Aggregation via Probe Enhancement–Fluorescence Correlation Spectroscopy

Journal

ACS Chemical Neuroscience, 6(9)

ISSN

1948-7193

Authors

Guan, Yinghua
Cao, Kevin J
Cantlon, Adam
et al.

Publication Date

2015-09-16

DOI

10.1021/acschemneuro.5b00176

Peer reviewed

ACS Chemical Neuroscience

Letter

pubs.acs.org/chemneuro

Real-Time Monitoring of Alzheimer's-Related Amyloid Aggregation via Probe Enhancement–Fluorescence Correlation Spectroscopy

Yinghua Guan,[†,‡] Kevin J. Cao,[∥] Adam Cantlon,[§] Kristyna Elbel,[∥] Emmanuel A. Theodorakis,[∥] Dominic M. Walsh,[§] Jerry Yang,*[,∥] and Jagesh V. Shah*[,†,‡]

[†]Department of Systems Biology, Harvard Medical School, Boston, Massachusetts 02115, United States

[‡]Renal Division, and [§]Laboratory for Neurodegenerative Research, Ann Romney Center for Neurologic Diseases, Brigham and Women's Hospital, Boston, Massachusetts 02115, United States

[∥]Department of Chemistry and Biochemistry, University of California at San Diego, La Jolla, California 92093-0358, United States

Supporting Information

ABSTRACT: This work describes the use of fluorescence correlation spectroscopy (FCS) and a novel amyloid-binding fluorescent probe, ARCAM **1**, to monitor the aggregation of the Alzheimer's disease-associated amyloid β-peptide (Aβ). ARCAM **1** exhibits a large increase in fluorescence emission upon binding to Aβ assemblies, making it an excellent candidate for probe enhancement FCS (PE-FCS). ARCAM **1** binding does not change Aβ aggregation kinetics. It also exhibits greater dynamic range as a probe in reporting aggregate size by FCS in Aβ, when compared to thioflavin T (ThT) or an Aβ peptide modified with a fluorophore. Using fluorescent burst analysis (via PE-FCS) to follow aggregation of Aβ, we detected soluble aggregates at significantly earlier time points compared to typical bulk fluorescence measurements. Autocorrelation analysis revealed the size of these early Aβ assemblies. These results indicate that PE-FCS/ARCAM **1** based assays can detect and provide size characterization of small Aβ aggregation intermediates during the assembly process, which could enable monitoring and study of such aggregates that transiently accumulate in biofluids of patients with Alzheimer's and other neurodegenerative diseases.

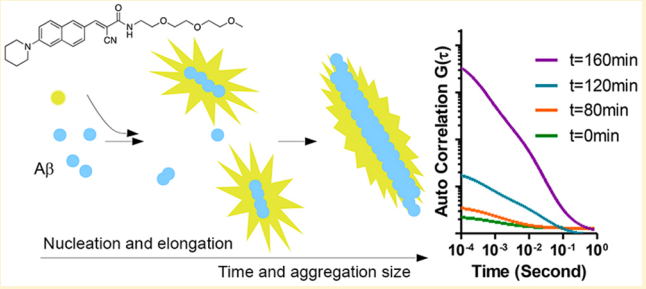

KEYWORDS: *Amyloid β-protein, Alzheimer's disease, aggregate-binding fluorescent probe, fluorescence correlation spectroscopy*

Aggregation and deposition of certain proteins is a common facet of many neurological disorders. Specifically, a defining feature of Alzheimer's disease pathology is the presence of abundant amyloid plaques, the principle component of which is the amyloid β-peptide (Aβ).[1] How the intrinsically disordered Aβ monomers convert to the fibrillar aggregates found in amyloid plaques and the relationship between Aβ aggregation and disease remain poorly understood.[2] However, it is widely believed that intermediates in Aβ aggregation, referred to as oligomers, are the initiators of a complex molecular cascade that, over a course of decades, leads to dementia.[3] To date, the real time study of Aβ aggregation in solution has been limited by methods that detect abundant assemblies of protofibrils and mature fibrils.[3]

Real time detection of aggregates typically relies upon the use of fluorophores, such as Thioflavin T (ThT), that are applied in bulk fluorescence measurement assays.[4] When ThT is introduced to a solution of amyloidogenic proteins or peptides, its emission intensity increases with increasing population of aggregates. A major limitation of amyloid aggregation assays that use ThT, however, is that the bulk fluorescence intensity increases above background only once protofibril and fibril structures have become abundant in solution, precluding the capability to detect small, transient intermediates.[4,5] Moreover, ThT has a significant fluorescence as an unbound dye, decreasing the signal-to-noise ratio for sensitive measurements of small assemblies.

Fluorescence correlation spectroscopy (FCS) is a time-resolved spectroscopic technique that can measure the concentration and size of fluorescently labeled particles.[6] This method has wide applications in the study of aggregation phenomena such as protein oligomerization (e.g., p53[7,8]) or formation of large aggregates such as prions.[9,10] FCS has also been used to study Aβ aggregation using fluorescently labeled peptides.[11−15] However, the effect of the fluorescent label covalently attached to the peptide on assembly dynamics in these prior studies remains unclear. Moreover, the need to incorporate exogenously added fluorescent Aβ peptides complicates the translation of data related to the detection of amyloid species in human biofluids such as cerebrospinal fluid.[15] In order to circumvent these limitations, we developed a novel fluorescent probe that undergoes strong fluorescence emission when bound to aggregates of amyloidogenic proteins and has a low unbound fluorescence. Fluorescence enhancement in the bound state can

Published: July 26, 2015

DOI: 10.1021/acschemneuro.5b00176
ACS Chem. Neurosci. 2015, 6, 1503−1508

dramatically increase the signal-to-noise and permit fluorescent intensity fluctuations (required for FCS measurements) that are derived primarily from amyloid-bound probe rather than unbound probe in solution. Here, we explore if this form of probe enhancement-FCS (PE-FCS), using the *aryl cyano amide* (ARCAM) **1** probe, can detect Aβ aggregates at earlier time points along the aggregation pathway in comparison to standard bulk fluorescence measurements.

We previously described a family of fluorescent probes that bind Aβ assemblies in solution and in tissue.[16−18] These probes exhibit a large enhancement in fluorescence properties when bound to aggregates compared to the weaker fluorescence of the unbound compounds in solution. For the experiments in this study, we designed and synthesized a novel Aβ aggregate-binding probe, ARCAM **1** (Figure 1A). This probe displayed an ∼8-fold

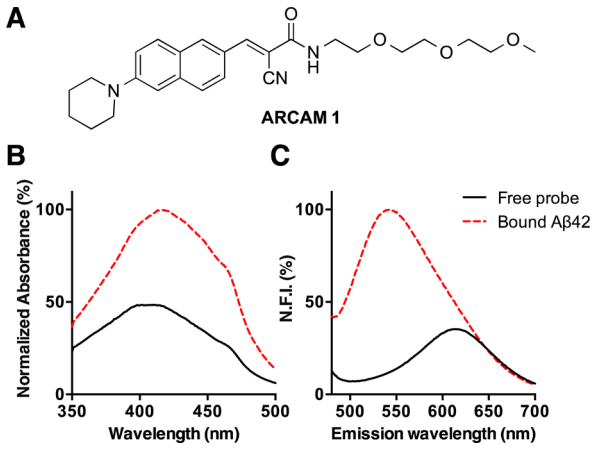

Figure 1. Structure and spectroscopic properties of fluorescent probe **1**. (A) Structures of fluorescent, aggregate-binding compound ARCAM **1**. Excitation (B) and emission (C) properties of **1** in the presence or absence of aggregated Aβ(1−42).

increase (at a λ_{em}(bound) of ∼540 nm) in fluorescence emission upon binding to aggregated Aβ in solution versus probe without Aβ (Figure 1C). The affinity of ARCAM **1** for aggregated Aβ (K_d = 870 ± 280 nM at pH 7.4) was comparable to the binding of similar fluorescent probes[18] (see Figure S1 in the Supporting Information). An important advantage of ARCAM **1** for aggregation studies is its stability in aqueous solutions (Figure S2) and broad insensitivity of fluorescence as a function of pH (Figure S3). For instance, the half-life of ARCAM **1** in phosphate buffered saline (PBS) at room temperature was ∼150 h. Importantly, there is negligible change in the effective concentration of ARCAM **1** over the aggregation time courses. In addition, ARCAM **1** shows similar multiphoton excitation (used in our FCS setup) to that of ThT (Figure S4).

To determine whether ARCAM **1** could be used to monitor Aβ (1−42) aggregation kinetics, we prepared a 10 μM solution of peptide monomers completely free of aggregates,[19,20] added ARCAM **1** and monitored total fluorescence at intervals until a stable maximal fluorescence was achieved. In parallel, an identical time course was monitored by ThT. Experiments were conducted at room temperature and were shaken in between sample readings (see the Supporting Information for details). ARCAM **1** and ThT time courses looked identical when the probe was present in solution throughout the aggregation process (see Figure S5).

Probe-enhancement FCS relies on the increase in fluorescence that occurs as a result of the probe binding to its target. To compare fluorescent probes for detecting Aβ aggregates, we measured FCS curves for solutions containing diluted, preaggregated Aβ and the probes. We added either ThT or ARCAM **1** to preaggregated Aβ samples (Figure S6). Separately, we added TAMRA-labeled Aβ (1−42) peptides or ARCAM **1** to another set of matched samples. FCS measurements of the probe-Aβ solutions were taken after a 30 min incubation at room temperature to permit probe binding (for ThT and ARCAM **1**) or monomer incorporation (for TAMRA-Aβ). Autocorrelation spectra of ThT-Aβ solutions showed the presence of primarily large aggregates, whereas ARCAM-Aβ solutions of the match sample showed a range of small and large aggregates (Figure 2A).

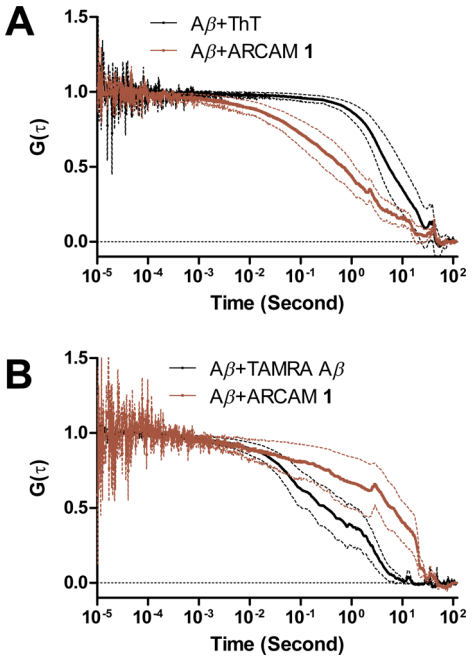

Figure 2. Comparison of aggregate size measured using ThT, ARCAM **1**, and fluorescently labeled Aβ peptide. Fluorescent probes (ThT or ARCAM **1**) or TAMRA-labeled Aβ(1−42) peptides were added to preaggregated Aβ samples. FCS measurements (shown with standard error of mean curves), after a 30 min incubation, revealed larger species in the ThT labeled sample (A, $p < 0.05$ for 0.1, 1 s delay time) compared to the ARCAM **1** labeled sample. ARCAM **1** revealed larger species in the preaggregated samples when compared to TAMRA-Aβ (1−42) peptides (B, $p < 0.05$ for 10 s delay time). Note that preaggregated samples were matched for measurements in (A) and (B) independently, resulting in the different ARCAM 1 FCS spectra.

Conversely, TAMRA-Aβ solutions showed small aggregates whereas measurements of the matched ARCAM **1**-Aβ solution showed a range of small and large aggregates (Figure 2B). Together, these point to ARCAM **1** detecting a larger dynamic range of aggregate sizes compared to ThT or TAMRA-labeled peptides, making it a useful choice for further studies by PE-FCS methods.

Bulk fluorescent measurements of an Aβ (1−42) aggregation time course (Figure 3A), in the presence of ARCAM **1** were also carried out in parallel with FCS measurements. Aliquots were collected at 20 min intervals and the samples were analyzed by multiphoton FCS.[7,10,21] The presence of bright fluorescent bursts in the intensity traces are indicative of aggregated amyloid species that were bound by ARCAM **1** diffusing through the

DOI: 10.1021/acschemneuro.5b00176
ACS Chem. Neurosci. 2015, 6, 1503−1508

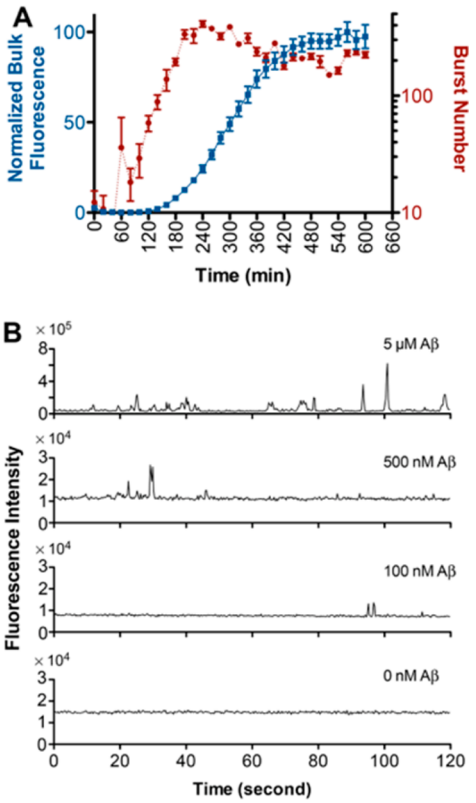

Figure 3. Monitoring the kinetics of aggregation of Aβ (1−42) peptides by bulk fluorescence and FCS burst analysis. (A) Increase in total fluorescence (blue squares) or fluorescent burst number (red squares) in solutions containing Aβ and fluorescent ARCAM **1**. (B) Detection of aggregates interacting with ARCAM **1** by monitoring the intensity and number of fluorescent bursts within a 120 s acquisition time window as a function of the concentration of total peptide (see the Supporting Information).

multiphoton excitation volume (Figure 3B and Figure S7). Burst analysis of these intensity traces counts the statistically significant events (intensity values in top 0.01%) in a fixed time window (see Supporting Information text and Figure S8 for details) to determine if ARCAM **1**-bound material is present in significant quantities. This analysis revealed the presence of ARCAM **1**-bound aggregated species at significantly earlier time points compared to aggregates that could be observed using bulk fluorescence measurements (Figure 3A, red circles compared to blue squares). Moreover, analysis of solutions of preformed aggregates (see Figure S6) revealed that the probe could detect aggregated species at total peptide concentrations as low as ∼100 nM (Figure 3B). Notably, solutions containing fluorescent ARCAM **1** alone (Figure 3B, bottom trace) or Aβ peptide alone (Figure S7) showed no fluorescence bursts by PE-FCS measurement.

In order to gain additional insight into the properties of the aggregates detected by PE-FCS, we also estimated the size of the species at the onset of increased burst activity (i.e., during the first 120 min of the aggregation of Aβ monomers, Figure 3A). To determine the size of the diffusing species, intensity time traces (e.g., Figure 3B) were subjected to autocorrelation analysis.[7,10] The result is a correlation function $G(\tau)$ that is proportional to the number of burst events while a molecule is resident in the excitation volume for the delay time, τ (Figure 4, and see the Supporting Information). The residence time is directly related to the translational diffusion constant and, therefore, its size.

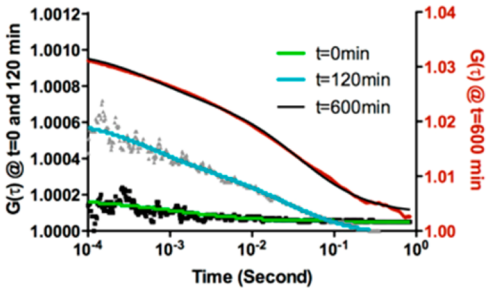

Figure 4. Representative raw FCS autocorrelation curves with fitting curves at three time points (t = 0, 120, and 600 min) are plotted together for comparison. Time points of t = 0 and 120 min share the same left y-axis, and the t = 600 min time point uses the right y-axis with a different scale. The amplitude of autocorrelation curve $G(0)$ increases along the reaction time point 0, 120, and 600 min, indicating a decrease in particle number for the dominant fluorescent species. The autocorrelation functions show increasing contribution from long delay times, indicating the increasing size of the particles.

For mixed species solutions, individual species sizes can be distinguished when they exhibit sufficiently different diffusion constants (∼5-fold difference in size). However, for more complex mixtures, FCS can only provide an average diffusion constant that is biased toward the more fluorescent species. In addition, the $G(0)$ point is inversely proportional to the number of particles in the solution. For ARCAM **1**-Aβ (1−42) solutions, there were two diffusing species: unbound ARCAM **1** and bound to Aβ. The FCS curve at time = 0 min was analyzed by a one component model (Figure S9), producing a diffusion coefficient (D1 = 148 ± 25 $\mu m^2/s$) consistent with the free diffusion of ARCAM **1**.[22] A two-component fitting model, to distinguish free dye from bound, was used for the analysis of the aggregation time series. Three representative FCS curves with fitting are shown in Figure 4 for different time points.

Time autocorrelation analysis of intensity fluctuations revealed diffusing assemblies with a mean diffusion constant of 3.42 $\mu m^2/s$ (range: 2.99−3.85 $\mu m^2/s$) at 120 min (Figure S9). This mean diffusion constant corresponds to a hydrodynamic radius between 64 and 82 nm in size for a spherical particle and 300−420 nm for an 8 nm diameter rod (see the Supporting Information). This hydrodynamic radius and proposed rod length are consistent with protofibrils, an early assembly intermediate in Aβ aggregation.[4]

We have, thus, demonstrated that the combination of a novel amyloid-binding fluorophore and FCS enabled the sensitive direct detection of amyloid assemblies at time points at earlier stages than conventional bulk fluorescence measurements. Here, we detected, in real time, amyloid aggregates that were only a few hundred nanometers in length, which is consistent in size with protofibrillar forms of Aβ intermediates.[3,4] Moreover, ARCAM **1** performed well in the detection of a large dynamic range of aggregate sizes in FCS measurements when compared to ThT or TAMRA-Aβ peptides. This PE-FCS method can detect low concentrations of early amyloid assembly intermediates that were consistent in size with a previous FCS study that used covalently labeled Aβ peptides.[11] A major advantage of the method reported in this work is that using an exogenously added fluorescence reporter (as opposed to fluorescently labeled peptides) may make it possible to analyze patient samples containing a large mixture of native aggregated species. The combination of a fluorescent reporter and PE-FCS-based detection of aggregated Aβ represents a potentially important

DOI: 10.1021/acschemneuro.5b00176
ACS Chem. Neurosci. 2015, 6, 1503−1508

step toward establishing a reliable method for studying aggregate intermediates that may be present in human cerebrospinal fluid.[23]

METHODS

Synthesis of ARCAM 1 (Scheme 1). *2-(2-(2-Methoxyethoxy)-ethoxy)ethyl 4-Methyl-benzene-sulfonate (**A**).* (Methoxyethoxy)-ethoxy ethanol (20.0 g, 0.122 mol) was added to a solution of dry pyridine (49.0 mL) and CH_2Cl_2 (152 mL). The solution was cooled to 0 °C and p-toluenesulfonyl chloride (27.9 g, 0.146 mol) was added in one portion with stirring. The reaction was allowed to come to room temperature and stir for 24 h. The reaction was then concentrated in vacuo, and the solution was filtered to remove solids. The filtrate was purified by flash silica column chromatography (0−3% MeOH/EtOAc) to give **A** (20.5 g, 53%) as a clear pale yellow oil. (A) R_f = 0.85 (9% MeOH/EtOAc). ^{1}H NMR (500 MHz, $CDCl_3$) δ 7.79 (d, J = 8.0 Hz, 2H), 7.33 (d, J = 8.0 Hz, 2H), 4.15 (m, 2H), 3.52−3.69 (m, 10H), 3.37 (s, 3H), 2.44 (s, 3H). ^{13}C (125 MHz, $CDCl_3$) δ 144.9, 133.0, 129.9, 128.1, 72.0, 72.0, 71.5, 70.9, 7038, 70.7, 70.7, 70.7, 69.4, 68.8, 59.2, 42.9, 21.8. HRMS calcd for $C_{14}H_{22}O_6SNa$ [M + Na]$^+$, 341.1029; found, 341.1030 by ESI.

*1-Azido-2-(2-(2-methoxyethoxy)ethoxy)ethane (**B**).* To a solution of **A** (1.0 g, 3.14 mmol) in DMF (125 mL) in a flask equipped with a condenser was added sodium azide (0.51 g, 7.85 mmol), and the reaction was heated to 67 °C for 15 h. The reaction was then cooled to room temperature, diluted with water (125 mL), and stirred for 30 min. The reaction mixture was poured into ice (150 mL) and extracted with diethyl ether (3 × 50 mL). The combined organic extracts were washed with water (2 × 30 mL) and dried with anhydrous $MgSO_4$. The solvent was then removed in vacuo, and the residue was purified via silica gel flash chromatography (10−70% EtOAc/hexanes) to give **B** (355 mg, 60%) as a clear colorless oil. (B) R_f = 0.6 (50% EtOAc/hexanes). ^{1}H NMR (500 MHz, $CDCl_3$) δ 3.65 (m 8H), 3.55−3.56 (m, 2H), 3.39−3.40 (m, 2H), 3.38 (s, 3H). ^{13}C (125 MHz, $CDCl_3$) δ 72.0, 70.8, 70.8, 70.2, 59.2, 50.8. HRMS calcd for $C_7H_{15}N_3O_3Na$ [M + Na]$^+$, 212.1006; found, 212.1006 by ESI.

*2-Cyano-N-(2-(2-(2-methoxyethoxy)ethoxy)ethyl)acetamide (**C**).* **B** (3.0 g, 15.7 mmol) was dissolved in diethyl ether (628 mL) and cooled to 0 °C. Triphenylphosphine (5.0 g, 18.8 mmol) was added in one portion, and the mixture was allowed to stir at 0 °C for 1 h and then at room temperature for 6 h. Water (200 mL) was then added and the reaction was allowed to stir for 12 h. Toluene (150 mL) was then added and the reaction was allowed to stir for an additional 12 h. The water layer was then isolated and washed with toluene (1 × 200 mL) and then removed in vacuum to give the corresponding amine as a clear yellow oil which, without further purification, was subjected to the next reaction. A solution of amine (1.79 g, 10.97 mmol), prepared as described above, and hydroxybenzotriazole (HOBt) (1.48 g, 10.97 mmol) in CH_2Cl_2 (10 mL) was added dropwise via syringe to a cold (0 °C) solution of cyanoacetic acid (0.621 g, 7.3 mmol) in CH_2Cl_2 (15 mL) under argon. The reaction mixture was then allowed to stir for 10 min at 0 °C. 1-Ethyl-3-(3-(dimethylamino)propyl)-carbodiimide (EDC) (2.1 g, 10.97 mmol) was then added in one portion, and the reaction was allowed to stir overnight at 0 °C. The reaction was then concentrated in vacuo and purified via silica gel flash chromatography (0−2% MeOH/CH_2Cl_2) to give **C** (1.4 g, 83%) as a clear yellow oil. (C): R_f = 0.36 (10% MeOH/EtOAc). ^{1}H NMR (500 MHz, $CDCl_3$) δ 7.04 (bs, 1H), 3.63−3.65 (m, 6H), 3.55−3.59 (m, 4H), 3.45−3.48 (m, 2H), 3.39 (s, 2H), 3.37 (s, 3H). ^{13}C (125 MHz, $CDCl_3$) δ 161.5, 114.8, 71.9, 70.6, 70.4, 70.2, 69.3, 59.0, 40.1, 25.9. HRMS calcd for $C_{10}H_{18}N_2O_4Na$ [M + Na]$^+$, 253.1159; found, 253.1161 by ESI.

*(E)-2-Cyano-N-(2-(2-(2-methoxyethoxy)ethoxy)-ethyl)-3-(6-(piperidin-1-yl)naphthalen-2-yl)acrylamide (ARCAM **1**).* To a solution of 6-(piperidin-1-yl)naphthalene-2-carbaldehyde[16] (0.15 g, 0.627 mmol) and **C** (0.115 g, 0.501 mmol) in THF (2.5 mL) was added piperidine (0.01254 mmol), and the reaction was heated to 50 °C for 16 h. The reaction was then concentrated in vacuo, adsorbed on to silica, and purified via silica gel flash chromatography (0−20% acetone/toluene) to give ARCAM **1** (138 mg, 61%) as an orange solid. ARCAM **1**: R_f = 0.25 (5% acetone/toluene). ^{1}H NMR (500 MHz, $CDCl_3$) δ 8.33 (s, 1H), 8.11 (s, 1H), 8.00−8.02 (dd, J = 8.5 Hz, 1.5 Hz, 1H), 7.69−7.71 (d, J = 9.5 Hz, 1H), 7.60−7.62 (d, J = 8.5 Hz, 1H), 7.24−7.26 (m, 1H), 7.01 (bs, 1H), 6.84 (m, 1H), 3.64−3.66 (m, 6H), 3.62−3.63 (m, 4H), 3.54−3.55 (m, 2H), 3.35 (s, 3H), 3.12−3.34 (m, 4H), 1.69 (m, 4H), 1.61−1.62 (m, 2H). ^{13}C (125 MHz, $CDCl_3$) δ 161.2, 152.9, 151.6, 137.2, 133.8, 130.3, 127.2, 126.6, 126.1, 125.7, 119.4, 117.8, 108.6, 100.5, 71.9, 70.6, 70.6, 70.5, 69.4, 59.0, 49.5, 40.2, 25.5, 24.3. HRMS calcd for $C_{26}H_{32}N_2O_5Na$ [M + Na]$^+$, 474.2363; found, 474.2363 by ESI.

Scheme 1. Synthesis of ARCAM 1[a]

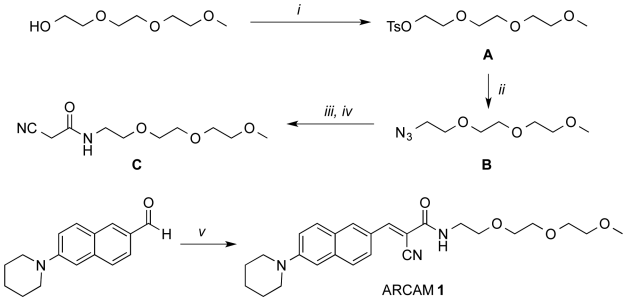

[a](i) *p*-TsCl, pyridine, DCM; (ii) NaN_3, DMF; (iii) PPh_3, Et_2O, H_2O; (iv) cyanoacetic acid, EDC, HOBt, DCM; (v) **C**, piperidine (cat), THF

Preparation of Aggregated Aβ(1−42). Aggregation of Aβ(1−42) was monitored using a continuous ThT assay, and material which exhibited maximal fluorescence (t_{max}) was used as our aggregate standard.[24,25] Briefly, solutions of Aβ(1−42) monomer were isolated as described in the Supporting Information, but in 10.9 mM HEPES pH 7.8, and diluted to 10 μM in the same buffer. A portion was held on ice and ThT added to the remainder to achieve a final concentration of 20 μM ThT. Aliquots (120 μL) of the peptide solutions were then dispensed into the wells of an ice-cold 96-well black microtiter plate (Nunc, Roskilde, Denmark) and read immediately. Plates were sealed with an adhesive plastic cover (WVR, Radnor, PA) and incubated at room temperature with shaking at 700 rpm in a VorTemp 56 shaker/incubator with an orbit of 3 mm (Labnet International, Windsor, U.K.). ThT fluorescence was measured every 20 min using a SpectraMax M2 microplate reader (Molecular Devices, Sunnyvale, CA) with excitation and emission of 435 and 485 nm, respectively. Aggregation was allowed to proceed until the maximal fluorescence reached a plateau (see Figure S6), then a portion of the same SEC-isolated monomer sample that had been held on ice was used for a repeat experiment exactly as described above, but adding an equal volume of Milli-Q water in place of ThT.

FCS Measurement of Preaggregated Aβ with ThT, ARCAM 1, and TAMRA-Aβ. ThT (20 μM) and ARCAM **1** (2.5 μM) were added into preaggregated Aβ (5 μM) for comparison or TAMRA-Aβ (2.5 μM, AnaSpec, Fremont, CA) and ARCAM **1** (2.5 μM) were added into preaggregated Aβ for comparison in FCS measurement.

Monitoring the Aggregation of Aβ(1−42) Using ARCAM 1 and bulk fluorescence measurements. Solutions of SEC-isolated Aβ(1−42) monomer were diluted to 10 μM with 20 mM ammonium bicarbonate pH 8.2 and ARCAM **1** was added to a final concentration of 2.5 μM. Aliquots (120 μL) of the peptide solutions were then dispensed into the wells of an ice-cold 96-well black microtiter plate (Nunc, Roskilde, Denmark) and read immediately. Plates were then sealed with an adhesive plastic cover (WVR, Radnor, PA) and incubated at room temperature with shaking at 500 rpm in a VorTemp 56 shaker/incubator with an orbit of 3 mm (Labnet International, Windsor, U.K.). The fluorescence of ARCAM **1** was measured every 20 min using a SpectraMax M2 microplate reader (Molecular Devices, Sunnyvale, CA) with excitation and emission of 410 and 570 nm, respectively. Data are presented as normalized bulk fluorescence plotted vs time.

Monitoring the Aggregation of Aβ(1−42) Using ARCAM 1 and FCS. Aggregation of Aβ(1−42) by FCS was monitored using a modified version of method used for bulk fluorescence measurements.

DOI: 10.1021/acschemneuro.5b00176
ACS Chem. Neurosci. 2015, 6, 1503−1508

Briefly, Aβ(1−42) monomers were diluted to 10 μM with 20 mM ammonium bicarbonate pH 8.2 and incubated in the presence of fluorescence probe at a final concentration of 2.5 μM. Aliquots (120 μL) of the peptide solutions were then dispensed into the wells of an ice-cold 96-well black microtiter plate (Nunc, Roskilde, Denmark) and read immediately. Plates were then sealed with an adhesive plastic cover (WVR, Radnor, PA) and incubated at room temperature with shaking at 500 rpm in a VorTemp 56 shaker/incubator with an orbit of 3 mm (Labnet International, Windsor, U.K.). Aliquots were removed every 20 min, and these aliquots were loaded onto microscope slides (treated with 0.1% BSA solution to reduce the nonspecific adsorption) and used for FCS.

FCS Setup and Data Analysis. FCS setup and data analysis were described as before.[7,10] For the burst analysis, the raw intensity traces were analyzed in the following four steps. First, the histogram of intensity trace (1 ms binning time windows) was plotted and the maximum peak (mode of the intensity trace) was used to designate the background signal (see Figure S8). The standard deviation (or width) of this histogram was also determined. Second, any signals from the trace with intensities greater than four times the width of the histogram above the background baseline (mode) were selected as burst candidates. Third, due to the diffusion properties, there may be bursts in rapid succession without any intervening time. We therefore merge these bursts as single burst event. Finally, based on the previous three steps, we generated a final burst trace that was used to calculate the burst number.

■ ASSOCIATED CONTENT

Supporting Information

The Supporting Information is available free of charge on the ACS Publications website at DOI: 10.1021/acschemneuro.5b00176.

Details for experimental protocols for binding, hydrolysis, bulk fluorescence, and FCS studies; supporting figures (PDF)

■ AUTHOR INFORMATION

Corresponding Authors

*E-mail: jagesh@hms.harvard.edu.

*E-mail: jerryyang@ucsd.edu.

Author Contributions

Y.G., K.J.C., A.C., K.E., E.A.T., D.M.W., J.Y. and J.V.S. designed research; Y.G., K.J.C., A.C. and K.E. performed research; Y.G., K.J.C., A.C., D.M.W., J.Y. and J.V.S. analyzed data; J.Y. and J.V.S. wrote the paper.

Funding

Financial support from the NIH [CA133002 (E.A.T.), AG046275 (D.W.)] and Beckman Laser Institute Foundation (Y.G., J.V.S.) is gratefully acknowledged.

Notes

The authors declare no competing financial interest.

■ ACKNOWLEDGMENTS

We would like to acknowledge the NIH for support of the Mass Spectrometry facility at UCSD (1S10RR25636-1A1).

■ REFERENCES

(1) Hardy, J., and Selkoe, D. J. (2002) The amyloid hypothesis of Alzheimer's disease: progress and problems on the road to therapeutics. *Science 297*, 353−356.

(2) Walsh, D. M., and Teplow, D. B. (2012) Alzheimer's disease and the amyloid beta-protein. *Progress in molecular biology and translational science 107*, 101−124.

(3) Benilova, I., Karran, E., and De Strooper, B. (2012) The toxic Abeta oligomer and Alzheimer's disease: an emperor in need of clothes. *Nat. Neurosci. 15*, 349−357.

(4) Walsh, D. M., Hartley, D. M., Kusumoto, Y., Fezoui, Y., Condron, M. M., Lomakin, A., Benedek, G. B., Selkoe, D. J., and Teplow, D. B. (1999) Amyloid beta-protein fibrillogenesis. Structure and biological activity of protofibrillar intermediates. *J. Biol. Chem. 274*, 25945−25952.

(5) Ban, T., Hamada, D., Hasegawa, K., Naiki, H., and Goto, Y. (2003) Direct observation of amyloid fibril growth monitored by thioflavin T fluorescence. *J. Biol. Chem. 278*, 16462−16465.

(6) Botvinick, E. L., and Shah, J. V. (2007) Laser-based measurements in cell biology. *Methods Cell Biol. 82*, 81−109.

(7) Gaglia, G., Guan, Y., Shah, J. V., and Lahav, G. (2013) Activation and control of p53 tetramerization in individual living cells. *Proc. Natl. Acad. Sci. U. S. A. 110*, 15497−15501.

(8) Rajagopalan, S., Huang, F., and Fersht, A. R. (2011) Single-Molecule characterization of oligomerization kinetics and equilibria of the tumor suppressor p53. *Nucleic Acids Res. 39*, 2294−2303.

(9) Bieschke, J., Giese, A., Schulz-Schaeffer, W., Zerr, I., Poser, S., Eigen, M., and Kretzschmar, H. (2000) Ultrasensitive detection of pathological prion protein aggregates by dual-color scanning for intensely fluorescent targets. *Proc. Natl. Acad. Sci. U. S. A. 97*, 5468−5473.

(10) Kayatekin, C., Matlack, K. E. S., Hesse, W. R., Guan, Y., Chakrabortee, S., Russ, J., Wanker, E. E., Shah, J. V., and Lindquist, S. (2014) Prion-like proteins sequester and suppress the toxicity of huntingtin exon 1. *Proc. Natl. Acad. Sci. U. S. A. 111*, 12085−12090.

(11) Matsumura, S., Shinoda, K., Yamada, M., Yokojima, S., Inoue, M., Ohnishi, T., Shimada, T., Kikuchi, K., Masui, D., Hashimoto, S., Sato, M., Ito, A., Akioka, M., Takagi, S., Nakamura, Y., Nemoto, K., Hasegawa, Y., Takamoto, H., Inoue, H., Nakamura, S., Nabeshima, Y., Teplow, D. B., Kinjo, M., and Hoshi, M. (2011) Two distinct amyloid beta-protein (Abeta) assembly pathways leading to oligomers and fibrils identified by combined fluorescence correlation spectroscopy, morphology, and toxicity analyses. *J. Biol. Chem. 286*, 11555−11562.

(12) Paredes, J. M., Casares, S., Ruedas-Rama, M. J., Fernandez, E., Castello, F., Varela, L., and Orte, A. (2012) Early Amyloidogenic Oligomerization Studied through Fluorescence Lifetime Correlation Spectroscopy. *Int. J. Mol. Sci. 13*, 9400−9418.

(13) Tjernberg, L. O., Pramanik, A., Bjorling, S., Thyberg, P., Thyberg, J., Nordstedt, C., Berndt, K. D., Terenius, L., and Rigler, R. (1999) Amyloid beta-peptide polymerization studied using fluorescence correlation spectroscopy. *Chem. Biol. 6*, 53−62.

(14) Mittag, J. J., Milani, S., Walsh, D. M., Radler, J. O., and McManus, J. J. (2014) Simultaneous measurement of a range of particle sizes during Abeta1−42 fibrillogenesis quantified using fluorescence correlation spectroscopy. *Biochem. Biophys. Res. Commun. 448*, 195−199.

(15) Pitschke, M., Prior, R., Haupt, M., and Riesner, D. (1998) Detection of single amyloid beta-protein aggregates in the cerebrospinal fluid of Alzheimer's patients by fluorescence correlation spectroscopy. *Nat. Med. 4*, 832−834.

(16) Sutharsan, J., Dakanali, M., Capule, C. C., Haidekker, M. A., Yang, J., and Theodorakis, E. A. (2010) Rational design of amyloid binding agents based on the molecular rotor motif. *ChemMedChem 5*, 56−60.

(17) Chang, W. M., Dakanali, M., Capule, C. C., Sigurdson, C. J., Yang, J., and Theodorakis, E. A. (2011) ANCA: A Family of Fluorescent Probes that Bind and Stain Amyloid Plaques in Human Tissue. *ACS Chem. Neurosci. 2*, 249−255.

(18) Cao, K., Farahi, M., Dakanali, M., Chang, W. M., Sigurdson, C. J., Theodorakis, E. A., and Yang, J. (2012) Aminonaphthalene 2-cyanoacrylate (ANCA) probes fluorescently discriminate between amyloid-beta and prion plaques in brain. *J. Am. Chem. Soc. 134*, 17338−17341.

(19) O'Malley, T. T., Oktaviani, N. A., Zhang, D., Lomakin, A., O'Nuallain, B., Linse, S., Benedek, G. B., Rowan, M. J., Mulder, F. A., and Walsh, D. M. (2014) Abeta dimers differ from monomers in structural propensity, aggregation paths and population of synaptotoxic assemblies. *Biochem. J. 461*, 413−426.

(20) Walsh, D. M., Hartley, D. M., Condron, M. M., Selkoe, D. J., and Teplow, D. B. (2001) In vitro studies of amyloid beta-protein fibril assembly and toxicity provide clues to the aetiology of Flemish variant (Ala692→Gly) Alzheimer's disease. *Biochem. J. 355*, 869−877.

DOI: 10.1021/acschemneuro.5b00176
ACS Chem. Neurosci. 2015, 6, 1503−1508

(21) Schwille, P., Haupts, U., Maiti, S., and Webb, W. W. (1999) Molecular dynamics in living cells observed by fluorescence correlation spectroscopy with one- and two-photon excitation. *Biophys. J. 77*, 2251−2265.
(22) Muller, J. D., Chen, Y., and Gratton, E. (2003) Fluorescence correlation spectroscopy. *Methods Enzymol. 361*, 69−92.
(23) Yang, T., Hong, S., O'Malley, T., Sperling, R. A., Walsh, D. M., and Selkoe, D. J. (2013) New ELISAs with high specificity for soluble oligomers of amyloid beta-protein detect natural Abeta oligomers in human brain but not CSF. *Alzheimer's Dementia 9*, 99−112.
(24) Betts, V., Leissring, M. A., Dolios, G., Wang, R., Selkoe, D. J., and Walsh, D. M. (2008) *Neurobiol. Dis. 31*, 442.
(25) Hellstrand, E., Boland, B., Walsh, D. M., and Linse, S. (2010) *ACS Chem. Neurosci. 1*, 13.

DOI: 10.1021/acschemneuro.5b00176
ACS Chem. Neurosci. 2015, 6, 1503−1508